Supporting Information

for

Preparation of graphene-encapsulated magnetic microspheres for protein/peptide enrichment and MALDI-TOF MS analysis

Qian Liu, Jianbo Shi, Mengting Cheng, Guoliang Li, Dong Cao, Guibin Jiang[*]

State Key Lab of Environmental Chemistry and Ecotoxicology, Research Center for Eco-Environmental Sciences,

Chinese Academy of Sciences, Beijing 100085, China

---

[*] Corresponding author. Email: gbjiang@rcees.ac.cn.

1. Experimental Section

1.1. Chemicals and reagents

Graphite powder (-325 mesh, 99.9995%) was bought from Alfa Aesar (Ward Hill, MA). Hydrazine hydrate (85%), P_2O_5, ethylene glycol and anhydrous ethanol were purchased from Sinopharm Chemical Reagent (Shanghai, China). H_2O_2, $KMnO_4$, $K_2S_2O_8$, H_2SO_4, $FeCl_3 \cdot 6H_2O$, toluene and polyethylene glycol (PEG 1000) were bought from Beijing Chemical Works (Beijing, China). C18 silica adsorbent was purchased from Supelco (Bellefonte, PA). Cytochrome c (Cyt c, from yeast) was from Sangon Biotech. (Shanghai, China). Myoglobin (Myo, from equine skeletal muscle), β-lactoglobulin (β-Lac, from bovine milk), bovine serum albumin (BSA), NaAc, 3-aminopropyltriethoxysilane (APTES) and tetraethylorthosilicate (TEOS) were from Sigma-Aldrich (St. Louis, MO). Trypsin (>2500 U/mg) was from Amresco (Solon, OH). α-Cyano-4-hydroxycinnamic acid (CHCA) was from Bruker Daltonics (Bremen, Germany). Acetonitrile (ACN) and trifluoroacetic acid (TFA) were from Dikma (Beijing, China) and of HPLC grade. Phosphate buffer saline (PBS) was from Thermo Hyclone (Logan, UT). Ultrapure water from Milli-Q system (Millipore, Billerica, MA) was used throughout. All reagents were of analytical grade unless otherwise noted.

1.2. Synthesis of graphene oxide (GO)

GO was synthesized using a modified Hummers method as described in previous reports.[1-3] Briefly, 3 g of graphite powder was pre-oxidized in 12 mL of H_2SO_4 containing 2.5 g of $K_2S_2O_8$ and 2.5 g of P_2O_5 at 80 ºC for 4.5 h, and then diluted with water and filtered through a 0.20 μm Millipore nylon membrane. The pre-oxidized product was added to 120 mL of H_2SO_4, and 15 g of $KMnO_4$ was slowly added with an ice-bath to keep the temperature below 20 ºC. The mixture was then stirred at 35 ºC for 2 h, followed by the addition of 250 mL of water with an ice-bath to keep the temperature below 50 ºC. Afterwards, the mixture was stirred for another 2 h and diluted with 0.7 L of water, and 20 mL of H_2O_2 (30%, v/v) was immediately added. The solid product was obtained via filtration and washed thoroughly with HCl and water. The as-synthesized graphite oxide was dispersed in water and ultrasonicated for 1 h to obtain a clear dispersion of GO.

1.3. Synthesis of Fe₃O₄@SiO₂@G

Firstly, Fe_3O_4 magnetic microspheres were synthesized by using Li's method.[4] $FeCl_3 \cdot 6H_2O$ (1.35 g) was dissolved in 40 mL of ethylene glycol, followed by the addition of 3.6 g of NaAc and 1.0 g of PEG 10000. The mixture was stirred vigorously for 30 min and then allowed to react at 200 °C for 8 h in a Teflon-lined stainless-steel autoclave. The Fe_3O_4 microspheres were collected by an external magnetic field, washed with ethanol and freeze-dried.

The Fe_3O_4 microspheres were then coated with silica shell by sol-gel process to prevent the microsphere from agglomeration and oxidization.[5, 6] Fe_3O_4 microspheres (600 mg) were dispersed in 50 mL of 2-propanol and 8 mL of water with the aid of ultrasonication. Then, 10 mL of ammonium hydroxide and 4 mL of TEOS were added in the dispersion, and the mixture was stirred at room temperature for 10 h. The product was washed with water and ethanol and freeze-dried. The obtained $Fe_3O_4@SiO_2$ was then dispersed in 50 mL of dry toluene, followed by the addtion of 0.5 mL of APTES. The mixture was refluxed for 24 h under nitrogen atmosphere to obtain amino-functionalized $Fe_3O_4@SiO_2$ ($Fe_3O_4@SiO_2-NH_2$). The product was washed with ethanol and freeze-dried.

To prepare $Fe_3O_4@SiO_2@GO$, 0.7 g of $Fe_3O_4@SiO_2-NH_2$ was dispersed in 100 mL of water with the aid of ultrasonication. Then, 100 mL of GO aqueous solution (0.5 mg/mL) was poured into the dispersion, and the mixture was stirred vigorously for 1 h at room temperature. The obtained $Fe_3O_4@SiO_2@GO$ was washed with water for several times and freeze-dried. $Fe_3O_4@SiO_2@G$ was synthesized via chemical reduction of $Fe_3O_4@SiO_2@GO$ by hydrazine. In a typical process, 0.5 g of $Fe_3O_4@SiO_2@GO$ was dispersed in 200 mL of water, and then 200 μL of hydrazine (85%) was added. The reaction was carried out at 95 °C for 1 h, and the final product was washed with water for several times and freeze-dried.

1.4. Characterization of materials

High-resolution STEM images were taken on a Hitachi S-5500 field-emission scanning electron microscope (Tokyo, Japan). Low-resolution SEM images were captured on a Hitachi S-3000N scanning electron microscope with an EDAX energy dispersive X-ray spectrometer (Mahwah, NJ). TEM images were captured on a Hitachi H-7500 transmission electron microscope. XPS spectra were obtained on an AXIS Ultra DLD X-ray photoelectron spectrometer (Kratos, Manchester, UK) with Al Kα X-ray radiation as the X-ray source excitation. XRD patterns were obtained on a PANalytical X'Pert PRO X-ray diffraction system (Almelo, Netherlands). Magnetic

hysteresis loops were measured on a VersaLab vibrating sample magnetometer (Quantum Design, San Diego, CA). Zeta potentials were measured on a Nano-ZS zetasizer (Malvern Instruments, Worcestershire, UK).

1.5. Adsorption test of proteins on $Fe_3O_4@SiO_2@G$

To test the adsorption kinetics of protein on $Fe_3O_4@SiO_2@G$, 4 mg of $Fe_3O_4@SiO_2@G$ was added to 500 μL of protein solution (0.05 mg/mL). The mixture was shaked at 37 °C for a period of time (5 – 120 min), and then $Fe_3O_4@SiO_2@G$ was separated on an 8-tube magnetic separation rack. The supernatant was collected and its UV-vis spectrum was measured on a Thermo Scientific Varioskan Flash multimode reader. The absorption at 408 nm was used for quantification of the protein. For adsorption isotherm, 2 mg of $Fe_3O_4@SiO_2@G$ was added to 500 μL of protein solution at concentrations ranging from 0.01 to 0.2 mg/g and shaked at 37 °C for 2 h. After magnetic separation, the absorption spectrum of the supernatant was examined. The amount of protein adsorbed was determined from the change in protein absorption at 408 nm. The data could be fitted to the Langmuir model.

1.6. Enrichment of protein and peptide samples

The protein and protein tryptic digest samples were prepared in PBS. In a typical enrichment process, 20 μL of $Fe_3O_4@SiO_2@G$ aqueous dispersion (20 mg/mL) was added to 500 μL of protein solution (500 nM) in a 1.5 mL centrifuge tube, and then the mixture was incubated in a shaker at 37 °C for 2 h to ensure equilibrium. The material was collected by magnetic separation and washed with 1 mL of water as a desalting step. Finally, 10 μL of 80% ACN/0.1% TFA was added into the tube and sonicated for 2 min to elute the protein. After magnetic separation, the supernatant was used for MALDI-TOF MS analysis. The material remained in the tube was washed with 100 μL of 80% ACN/0.1% TFA and 100 μL of water. In this way, the material was immediately available for the next use. For protein digest samples and those enriched using other materials, a similar enrichment process was adopted. When using C18 silica as adsorbent, the adsorbent was collected by centrifugation at 12000 rpm for 5 min.

1.7. Preparation of tryptic digests of BSA

The tryptic digests of BSA were prepared as follows:[7] firstly, the BSA solution was prepared in 50 mM Tris-HCl buffer (pH 8.5) at 10 mg/mL. For tryptic digestion, 20 μL of the trypsin solution

(10 mg/mL) prepared in 50 mM acetic acid was added to 500 µL of the BSA solution, and the mixture was incubated at 37 ºC for 20 h. Before enrichment and MS analysis, 50 µL of the BSA digest was diluted to 100 mL with PBS.

1.8. MALDI-TOF MS

MALDI-TOF MS analysis was performed on a Bruker Daltonics Autoflex III Smartbean MALDI-TOF mass spectrometer controlled by FlexControl software. Linear and reflector mode were used for the analysis of proteins and peptides, respectively. CHCA (10 mg/mL) dissolved in 50% ACN/0.1% TFA was used as matrix. For MS analysis, 0.5 µL of sample was mixed with 0.5 µL of the matrix, and the mixture was placed on a stainless steel MTP target frame III (Bruker Daltonics). A 337 nm nitrogen laser with the frequency of 100 Hz was used, and the laser power was set to 90% for proteins and 80% for peptides. The spectra were recorded by summing 200 laser shots for proteins and 500 laser shots for peptides. The system was calibrated using the peptide calibration standard from Bruker Daltonics, and the data processing was performed with the FlexAnalysis 3.0 software. For protein tryptic digest samples, the peptide peaks were identified according to ProteinProspector or IonSource databases.[8]

1.9. Analysis of biological samples

Saliva samples were collected from a healthy adult and diluted with PBS by 2-fold. The diluted saliva samples were centrifuged at 3500 rpm for 10 min, and the supernatant fraction was used for MALDI-TOF MS analysis. The enrichment process of the saliva samples were the same as stated in Section 1.6.

2. Supporting Tables

Table S1. Peptides identified from the BSA tryptic digest in the Fig. 3[a]

Number	m/Z	Sequence	pI[b]
1	841.46	LCVLHEK	6.7
2	1362.67	SLHTLFGDELCK	5.3
3	1386.62	YICDNQDTISSK	4.2
4	1479.79	LGEYGFQNALIV**R**	6.0
5	1519.75	LKPDPNTLCDEFK	4.6
6	1639.94	KVPQVSTPTLVEVSR	8.8
7	1823.90	**R**PCFSALTPDETYVPK	6.1

[a] The enrichment efficiency of peptides showed no clear relationship with pI. However, we noted that both the two highest peaks in Fig. 3 were arginine-terminated peptides (No. 4 and 7). Considering that arginine carries more positive charges than other amino acids, Fe_3O_4@SiO_2@G may have a stronger affinity for arginine-terminated peptides due to stronger electrostatic interaction.

[b] The pIs of peptides were calculated by Compute pI/Mw at http://web.expasy.org/compute_pi/.

Table S2. Recoveries and detection limits (LODs) of proteins for $Fe_3O_4@SiO_2@G$ and C18 adsorbents[a]

Protein	$Fe_3O_4@SiO_2@G$		C18	
	Recovery (%)[b]	LOD (fmol)[c]	Recovery (%)[b]	LOD (fmol)[c]
Cyt c	101.2 ± 6.7	3.8	86.4 ± 13.3	2.5
Myo	75.3 ± 1.9	6.3	49.9 ± 6.7	10.0
β-Lac	58.2 ± 6.0	68	15.8 ± 6.6	2.5×10^2

[a] The amount of adsorbents used was 0.4 mg for both $Fe_3O_4@SiO_2@G$ and C18. From Table S2, it can be seen that $Fe_3O_4@SiO_2@G$ was more efficient than C18 in enrichment of proteins, and the recoveries obtained with $Fe_3O_4@SiO_2@G$ were evidently higher than those with C18. Especially for β-Lac, its enrichment efficiency on C18 was rather poor. The LODs of Cyt c and Myo obtained with $Fe_3O_4@SiO_2@G$ and C18 were at the same level; while for β-Lac, $Fe_3O_4@SiO_2@G$ yielded a much lower LOD than C18.

[b] Assuming that the enrichment factor was 50 (500 to 10 μL), the recoveries were obtained by comparing the MS signals of 500 nM protein samples after enrichment with those of 25 μM protein samples prepared in pure water.

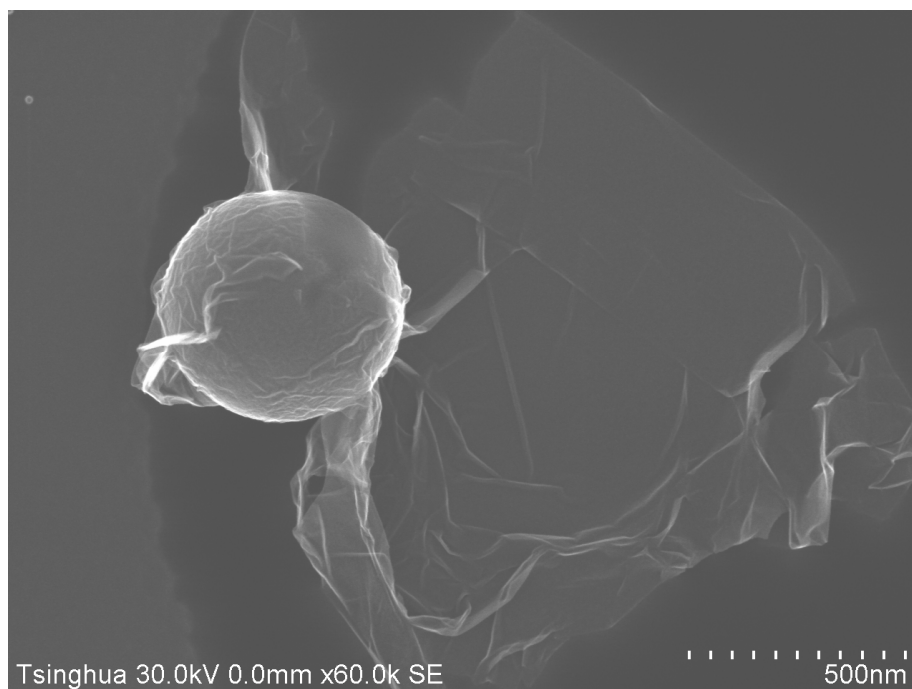[c] The LODs were estimated at S/N = 3.

3. Supporting Figures

Figure S1. Field-emission SEM (FE-SEM) image of a single $Fe_3O_4@SiO_2@G$ particle. It can be seen that the edges of G sheets could spread out of the spheres to a large extent with no conglomeration, thus keeping the high surface area of G and providing plenty of sites for adsorption.
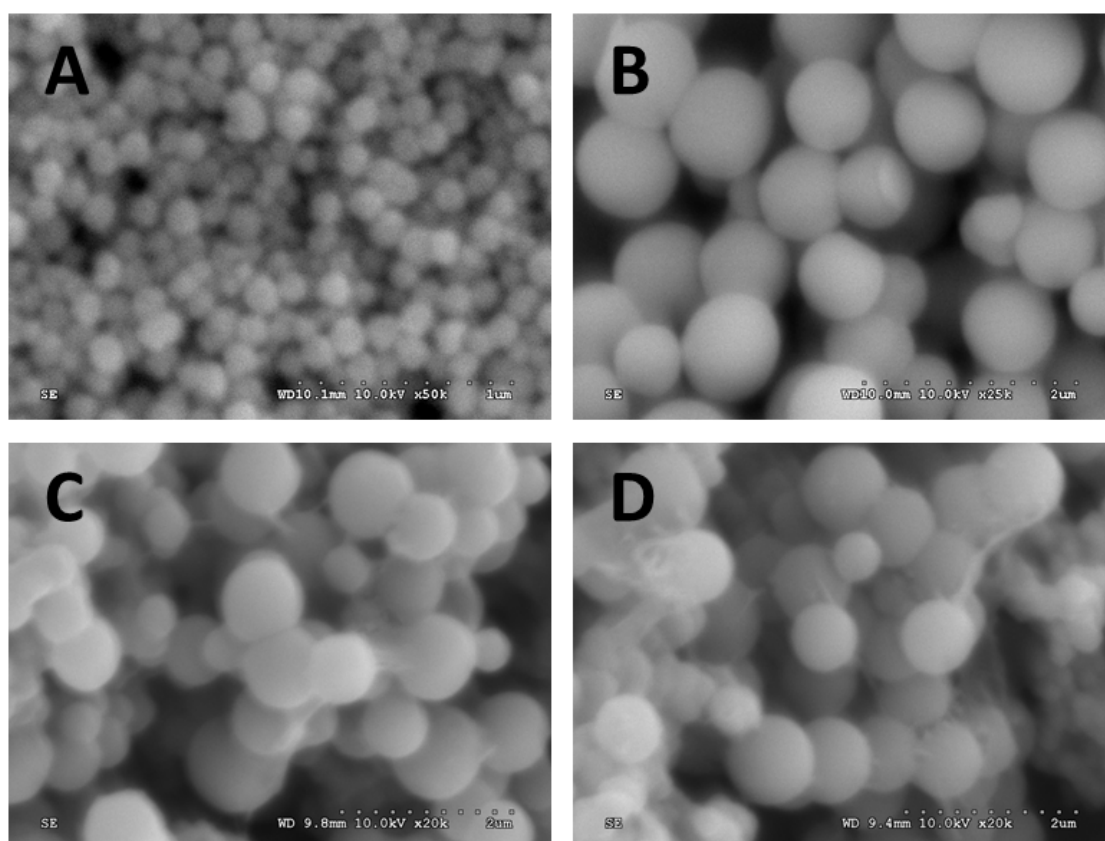
Figure S2. SEM images of (**A**) Fe_3O_4, (**B**) $Fe_3O_4@SiO_2$, (**C**) $Fe_3O_4@SiO_2@GO$, and (**D**) $Fe_3O_4@SiO_2@G$ microspheres. From (**A**), the as-synthesized Fe_3O_4 magnetic microspheres were near-monodispersed, and the average size was ca. 140 nm. From (**B**), after coated with silica, the average size of the magnetic microspheres increased to ca. 600 nm. (**C**) clearly shows that the $Fe_3O_4@SiO_2@GO$ spheres were closely encapsulated by GO sheets. The neighboring spheres were linked together by the flexible and ultrathin GO sheets. From (**D**), after chemical reduction, the microspheres were still encapsulated by G sheets, and no obvious change in morphology was observed.
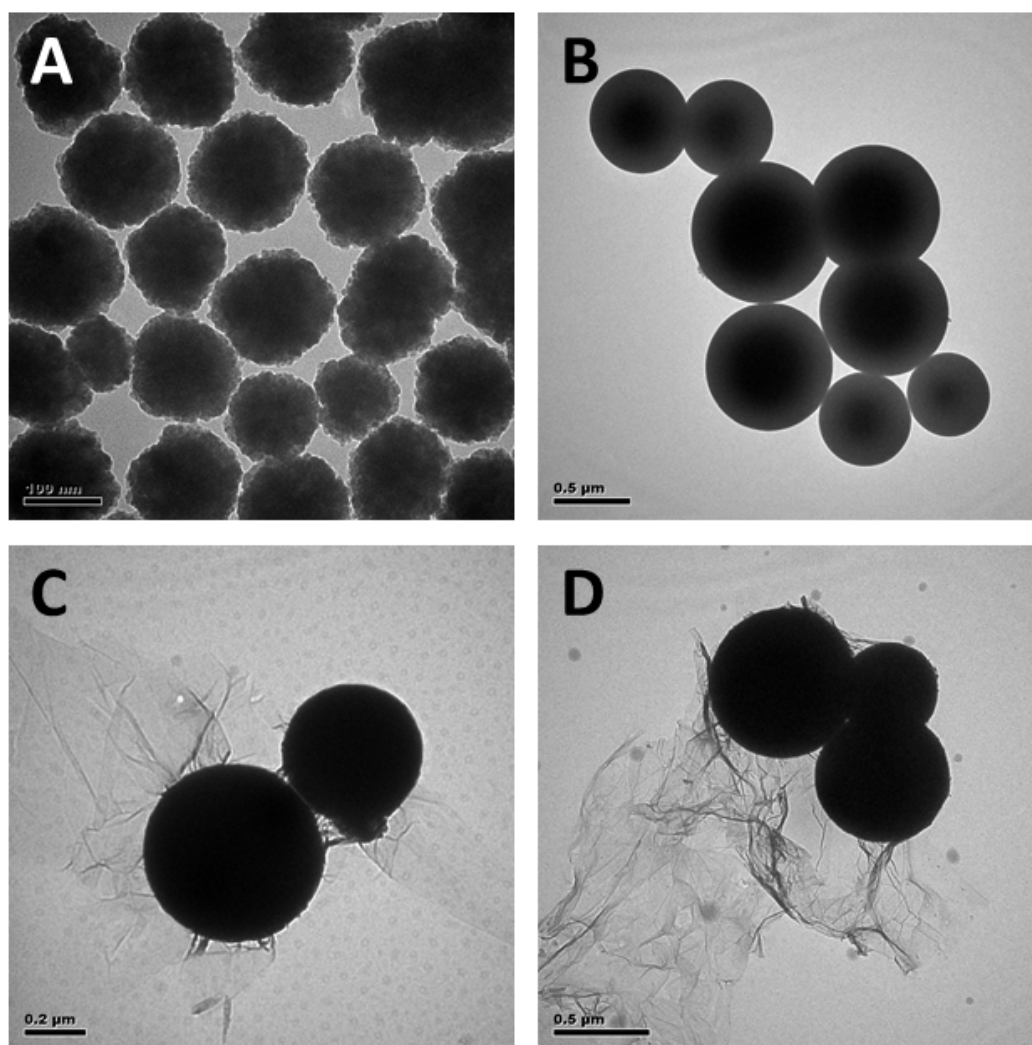
Figure S3. TEM images of (**A**) Fe$_3$O$_4$, (**B**) Fe$_3$O$_4$@SiO$_2$, (**C**) Fe$_3$O$_4$@SiO$_2$@GO, and (**D**) Fe$_3$O$_4$@SiO$_2$@G microspheres. (**C**) and (**D**) clearly show that the microspheres were tightly wrapped by the corrugated and ultrathin GO and G sheets. Particularly, the edges of G sheets extend out of the spheres, providing plenty of sites for adsorption.
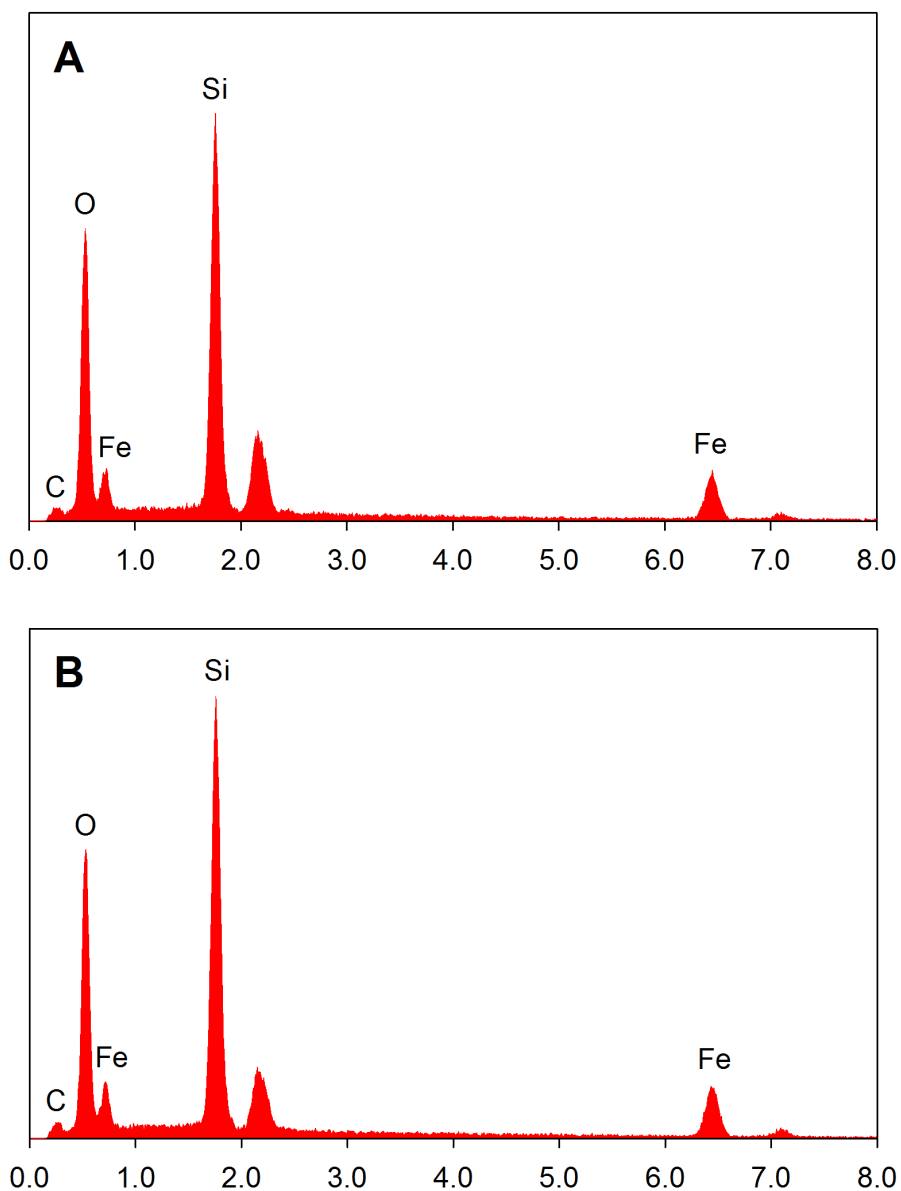
Figure S4. EDX images of (**A**) $Fe_3O_4@SiO_2$ and (**B**) $Fe_3O_4@SiO_2@G$. Compared with $Fe_3O_4@SiO_2$, $Fe_3O_4@SiO_2@G$ shows a slight enhancement in the intensity of C peak, indicating the introduction of G sheets to the surface of spheres.
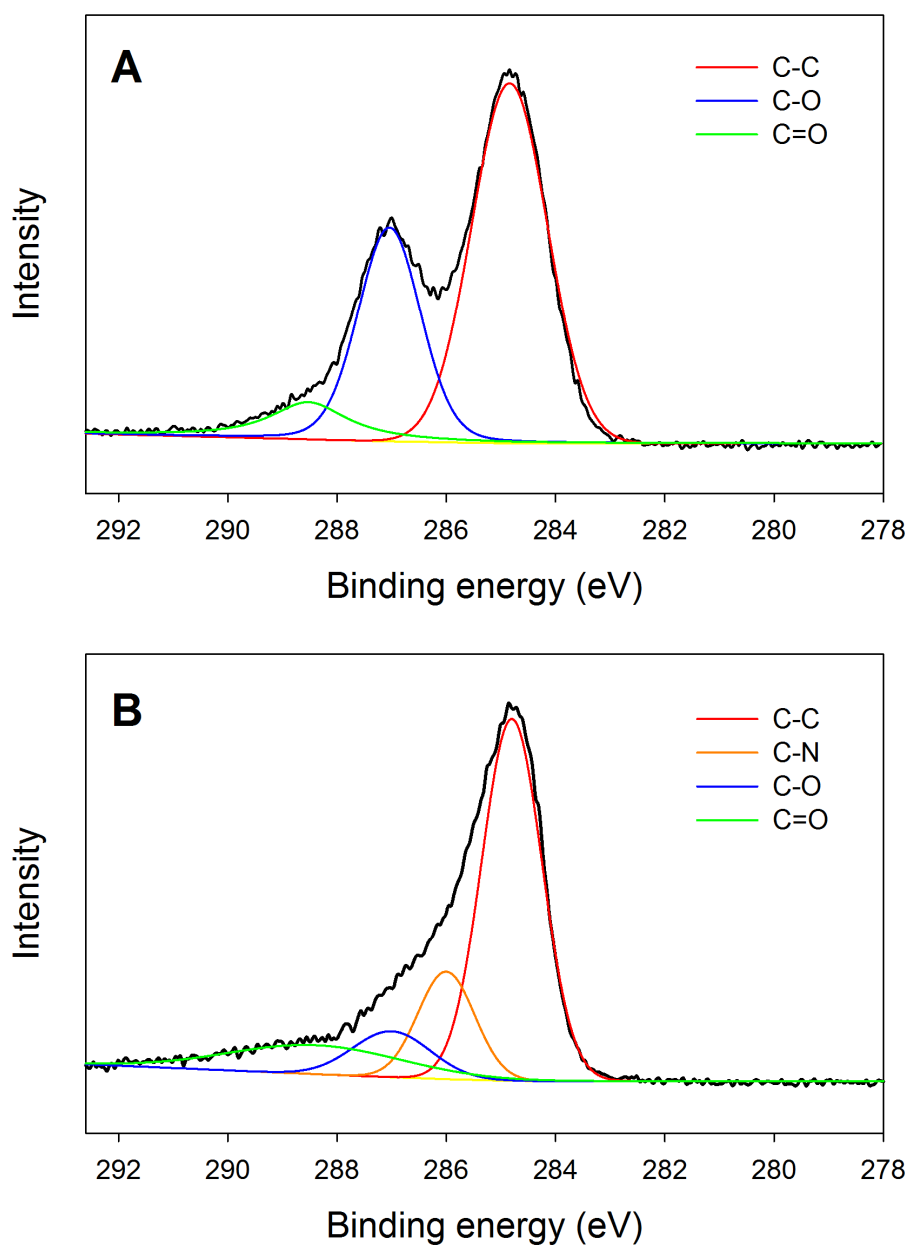
Figure S5. C1s XPS spectra of (**A**) $Fe_3O_4@SiO_2@GO$ and (**B**) $Fe_3O_4@SiO_2@G$. For $Fe_3O_4@SiO_2@GO$, peak fitting of the C1s bands yields three main components, i.e., C-C, C-O and C=O bonds, due to the presence of GO. After chemical reduction by hydrazine, the peak intensities of oxygen functionalities were remarkably reduced, and a new component corresponding to C-N bond was observed,[9] indicating the successful reduction of GO to G at the surface of the spheres.
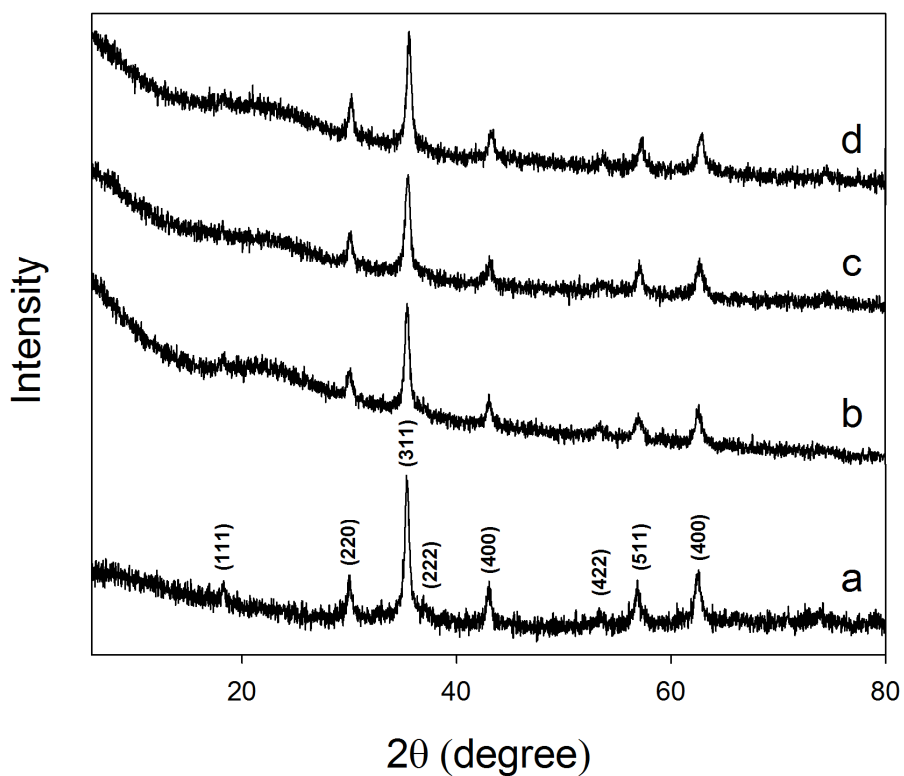
Figure S6. XRD patterns of (**a**) Fe$_3$O$_4$, (**b**) Fe$_3$O$_4$@SiO$_2$, (**c**) Fe$_3$O$_4$@SiO$_2$@GO, and (**d**) Fe$_3$O$_4$@SiO$_2$@G. All the patterns can be easily indexed to Fe$_3$O$_4$ (JCPDS 75-1609), indicating that the crystalline structure of Fe$_3$O$_4$ kept unchanged during the synthesis process of Fe$_3$O$_4$@SiO$_2$@G.
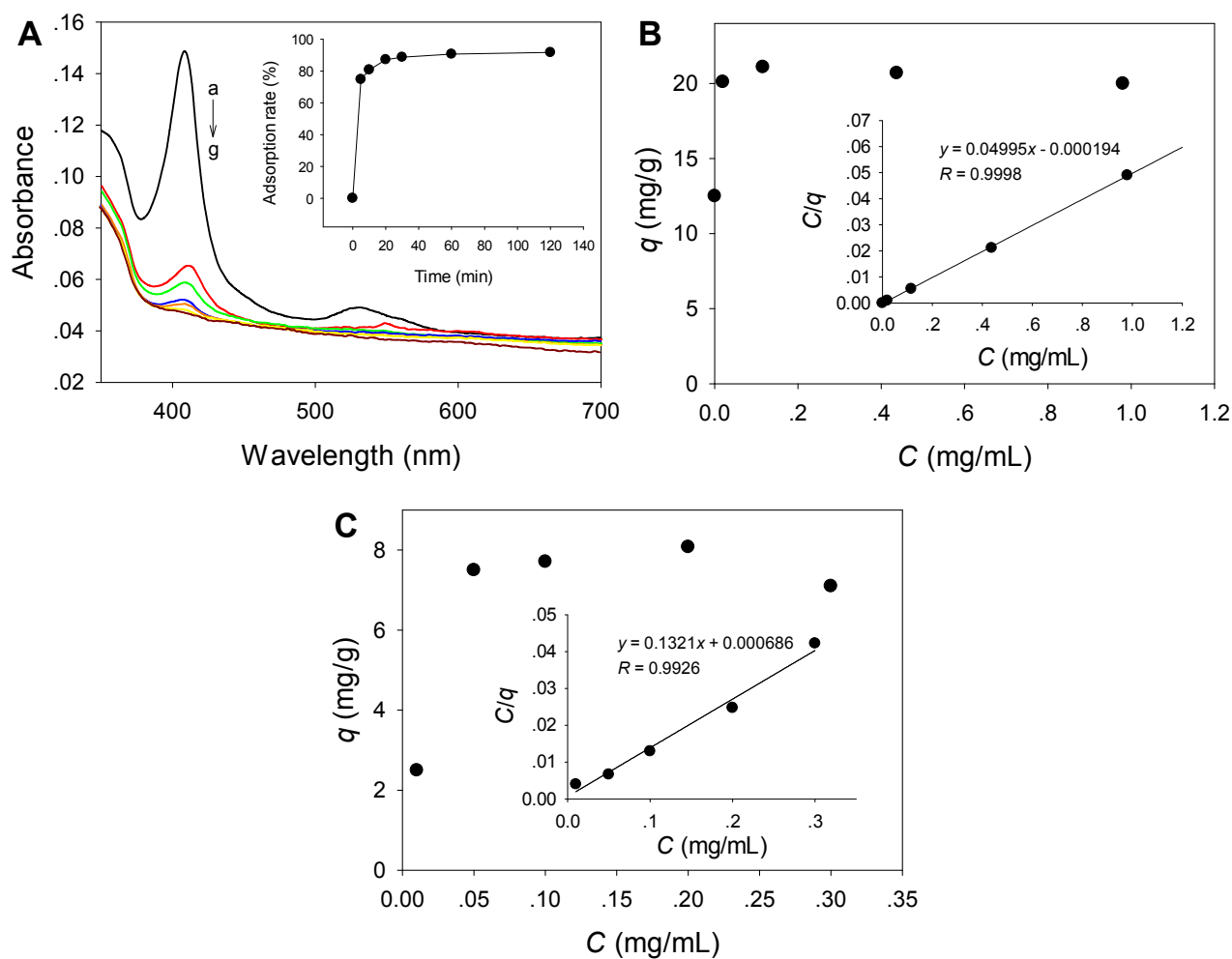
Figure S7. (**A**) UV-visible spectra of 4 μM Cyt c solution after adsorption by 4 mg of Fe$_3$O$_4$@SiO$_2$@G for 0 min (**a**), 5 min (**b**), 10 min (**c**), 20 min (**d**), 30 min (**e**), 1 h (**f**), and 2 h (**g**). The inset shows the kinetics curve of adsorption of Cyt c on Fe$_3$O$_4$@SiO$_2$@G. As shown, the adsorption of protein on Fe$_3$O$_4$@SiO$_2$@G is a relatively fast process. (**B**) Adsorption isotherm of Cyt c on Fe$_3$O$_4$@SiO$_2$@G. The inset was the linearized Langmuir plot.[10] C is the Cyt c concentration in equilibrium, and q is the amount of Cyt c adsorbed on Fe$_3$O$_4$@SiO$_2$@G (given in mg/g). The maximum adsorption capacity that was calculated from reciprocal slope of the straight line was 20.02 mg/g. (**C**) Adsorption isotherm of Cyt c on commercial C18 silica and the corresponding linearized Langmuir plot (the inset). The maximum adsorption capacity of Cyt c on C18 silica was calculated to be 7.57 mg/g.
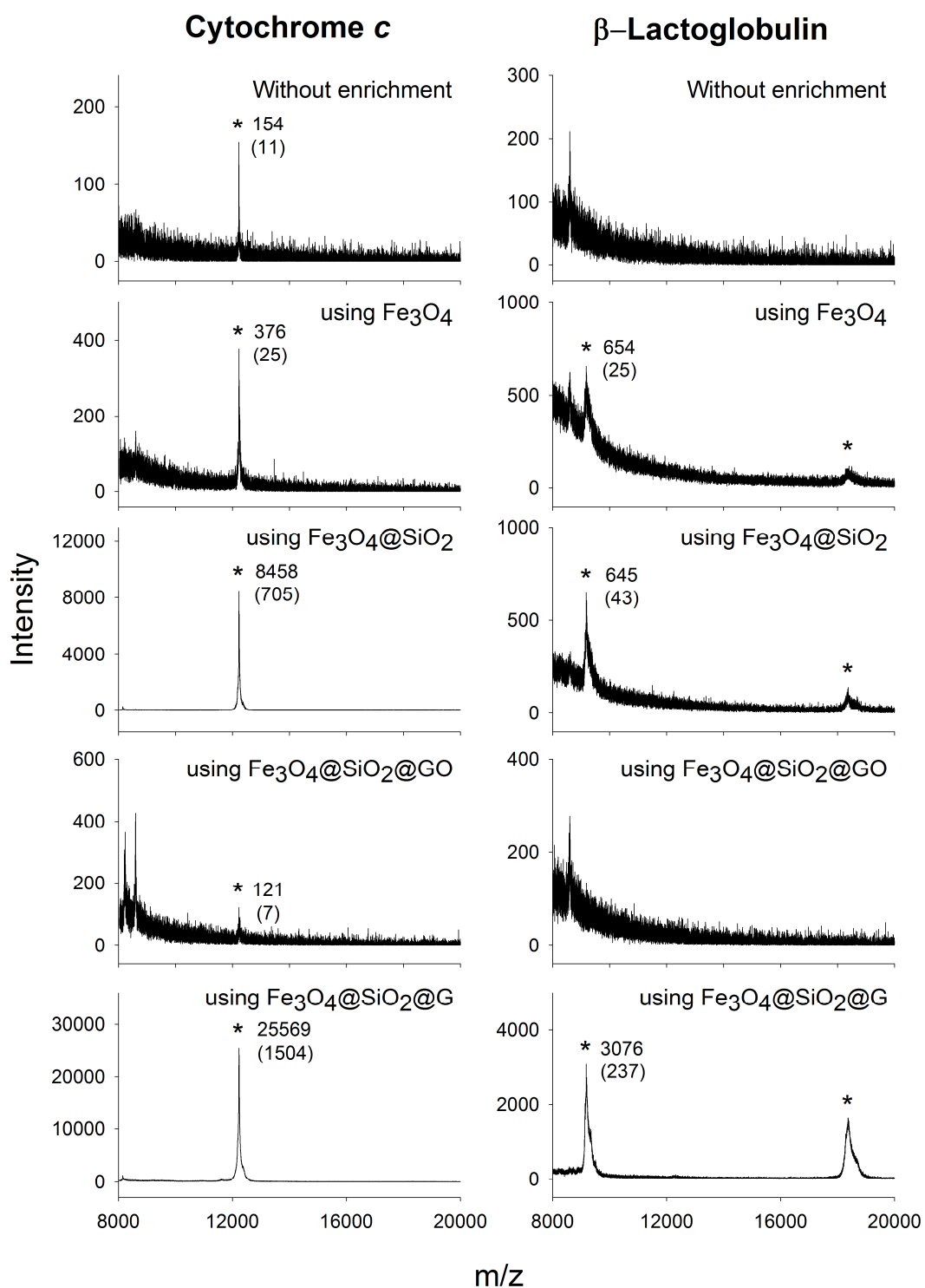
Figure S8. MALDI-TOF MS analysis of 500 nM Cyt *c* (left column) and 500 nM β-Lac (right column) samples without enrichment and those enriched by different materials. The feature peaks of the target molecules are marked by asterisks. The peak intensity and S/N ratio (in parentheses) are labelled for the highest peaks. As shown, the signals of the proteins were greatly enhanced after enrichment using $Fe_3O_4@SiO_2@G$ (the S/N ratios were increased by over two orders of magnitude). Furthermore, $Fe_3O_4@SiO_2@G$ yielded much higher enrichment factor than other materials.
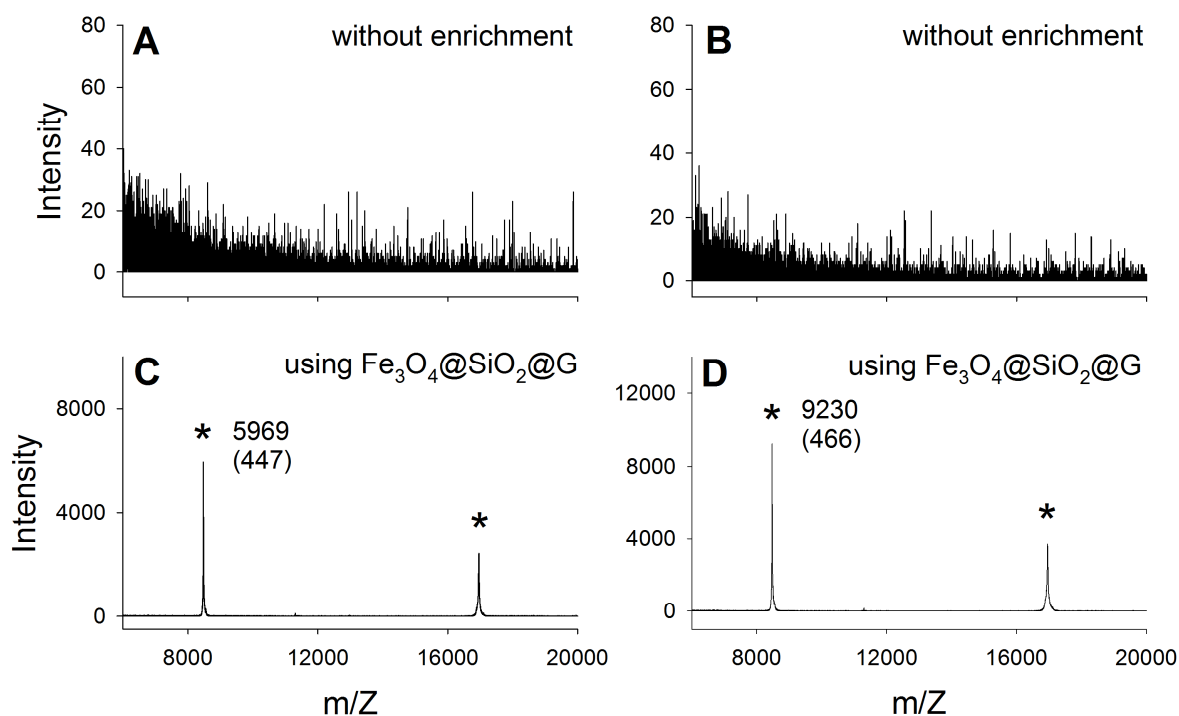
Figure S9. Enrichment of 500 nM Myo samples at different solution pHs by using $Fe_3O_4@SiO_2@G$. Sample: 500 nM Myo in 50 mM acetate buffer at pH 5.2 (**A**, **C**), and 500 nM Myo in 50 mM Tris-HCl buffer at pH 8.5 (**B**, **D**). As shown, without enrichment (**A**, **B**), no signals of protein could be observed. After being enriched by $Fe_3O_4@SiO_2@G$ (**C**, **D**), the signals were greatly enhanced at both pH values. Similar results have also been obtained for Cyt c and β-Lac (not shown). This revealed the robustness of this material for the use at different pH values.
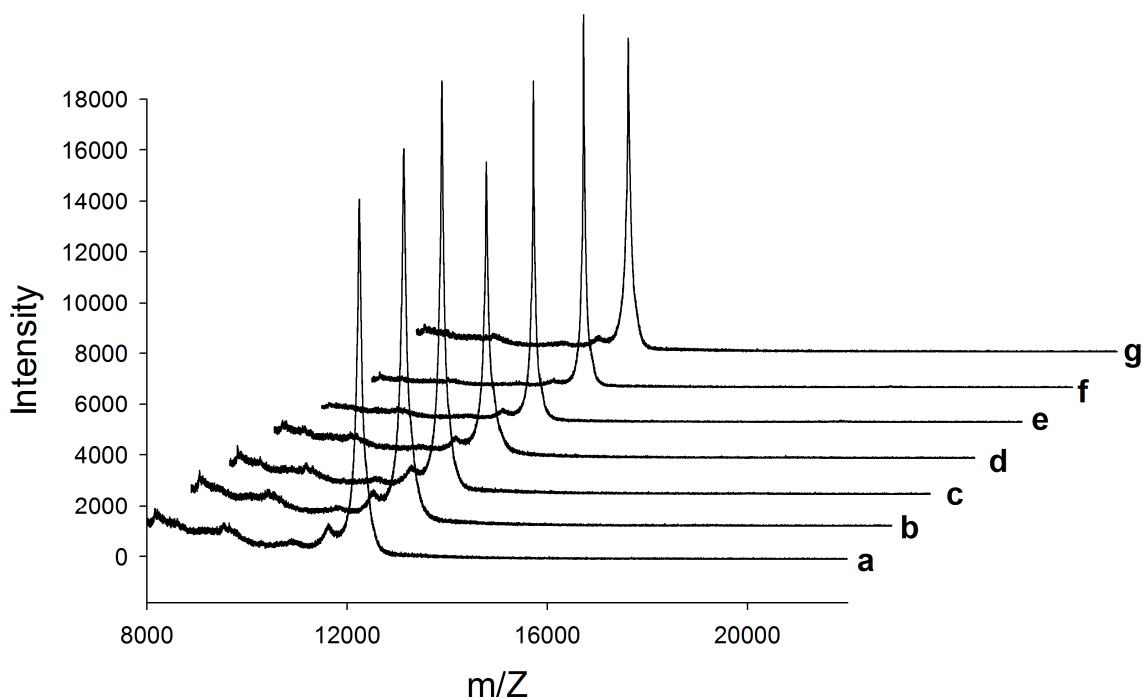
Figure S10. Reusability test of $Fe_3O_4@SiO_2@G$ in enrichment of 200 nM Cyt *c* samples. (**a** - **h**) represent the 1st to 7th reuse of the material. After each use, the $Fe_3O_4@SiO_2@G$ was recycled by washing with 100 μL of 80% ACN/0.1% TFA and 1 mL of water. No protein residuals were found on the recycled $Fe_3O_4@SiO_2@G$ examined by MALDI-TOF MS, indicating that the recycled microspheres were clean and immediately available for the next use. As shown, no deterioration in analysis performance was observed during the successive eight extractions using the same material, indicating that the material was reusable for protein enrichment.
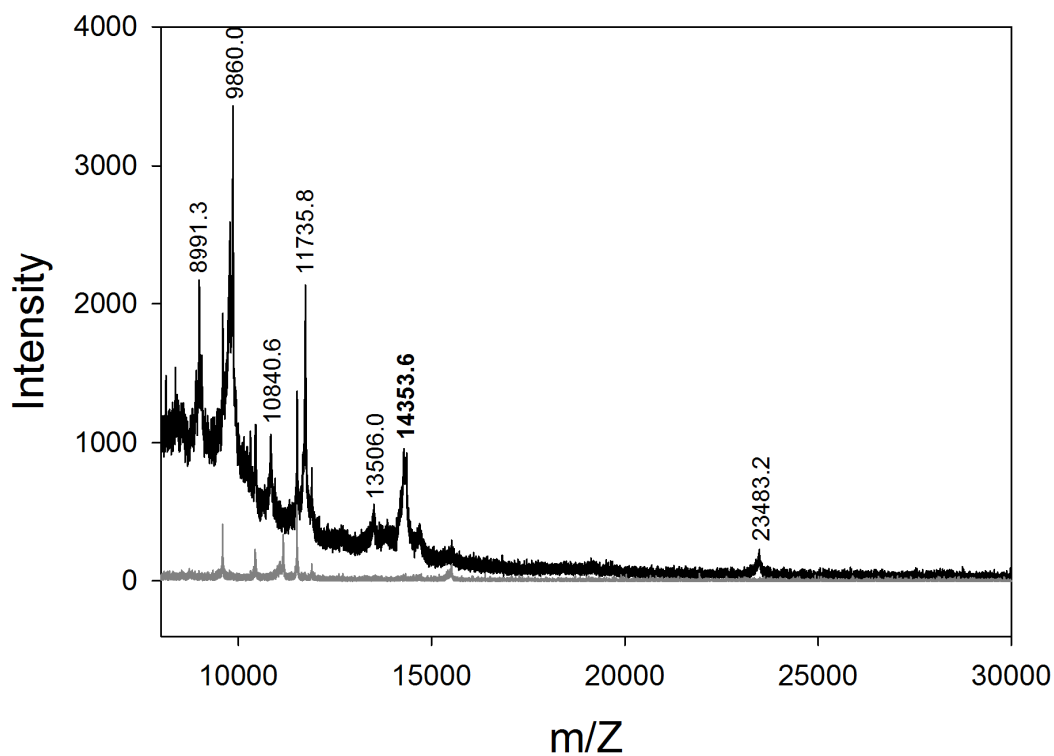
Figure S11. MALDI-TOF MS analysis of saliva samples after (black curve) and before (gray curve) enrichment by using $Fe_3O_4@SiO_2@G$. After enrichment, the signal intensity was greatly increased, and lysozyme (14353.6 $[M+H]^+$) could be easily identified, which was a major salivary protein. While without enrichment, no peak of lysozyme could be observed. Other proteins were not identified.

References

1   W. S. Hummers and R. E. Offeman, *J. Am. Chem. Soc.*, 1958, **80**, 1339.

2   Q. Liu, J. Shi, L. Zeng, T. Wang, Y. Cai and G. Jiang, *J. Chromatogr. A*, 2011, **1218**, 197.

3   Y. X. Xu, H. Bai, G. W. Lu, C. Li and G. Q. Shi, *J. Am. Chem. Soc.*, 2008, **130**, 5856.

4   H. Deng, X. L. Li, Q. Peng, X. Wang, J. P. Chen and Y. D. Li, *Angew. Chem. Int. Ed.*, 2005, **44**, 2782.

5   P. Tartaj and C. J. Serna, *J. Am. Chem. Soc.*, 2003, **125**, 15754.

6   F. Yang, Y. M. Long, R. Shen, C. Y. Chen, D. Pan, Q. L. Zhang, Q. Y. Cai and S. Z. Yao, *J. Sep. Sci.*, 2011, **34**, 716.

7   S. R. Liu, L. Gao, Q. S. Pu, J. J. Lu and X. J. Wang, *J. Proteome Res.*, 2006, **5**, 323.

8   http://prospector.ucsf.edu/prospector/mshome.htm; http://www.ionsource.com/.

9   S. Stankovich, D. A. Dikin, R. D. Piner, K. A. Kohlhaas, A. Kleinhammes, Y. Jia, Y. Wu, S. T. Nguyen and R. S. Ruoff, *Carbon*, 2007, **45**, 1558.

10   R. M. Vallant, Z. Szabo, S. Bachmann, R. Bakry, M. Najam-ul-Haq, M. Rainer, N. Heigl, C. Petter, C. W. Huck and G. K. Bonn, *Anal. Chem.*, 2007, **79**, 8144.